ADVANCES IN ATMOSPHERIC SCIENCES, VOL. 27, NO. 3, 2010, 455–468

Influences of Freshwater from Major Rivers on Global Ocean Circulation and Temperatures in the MIT Ocean General Circulation Model

Boyin HUANG* and Vikram M. MEHTA

The Center for Research on the Changing Earth System, Clarksville, Maryland 21029*, USA*

(Received 22 January 2009; revised 2 June 2009)

ABSTRACT

Responses of global ocean circulation and temperature to freshwater runoff from major rivers were studied by blocking regional runoff in the global ocean general circulation model (OGCM) developed at the Massachusetts Institute of Technology. Runoff into the tropical Atlantic, the western North Pacific, and the Bay of Bengal and northern Arabian Sea were selectively blocked. The blocking of river runoff first resulted in a salinity increase near the river mouths (2 practical salinity units). The saltier and, therefore, denser water was then transported to higher latitudes in the North Atlantic, North Pacific, and southern Indian Ocean by the mean currents. The subsequent density contrasts between northern and southern hemispheric oceans resulted in changes in major ocean currents. These anomalous ocean currents lead to significant temperature changes (1°C –2°C) by the resulting anomalous heat transports. The current and temperature anomalies created by the blocked river runoff propagated from one ocean basin to others via coastal and equatorial Kelvin waves. This study suggests that river runoff may be playing an important role in oceanic salinity, temperature, and circulations; and that partially or fully blocking major rivers to divert freshwater for societal purposes might significantly change ocean salinity, circulations, temperature, and atmospheric climate. Further studies are necessary to assess the role of river runoff in the coupled atmosphere-ocean system.

Key words: river runoff, ocean general circulation, freshwater flux

Citation: Huang, B., and V. M. Mehta, 2010: Influences of freshwater from major rivers on global ocean circulation and temperatures in the MIT ocean general circulation model. *Adv. Atmos. Sci.*, **27**(3), 455–468, doi: 10.1007/s00376-009-9022-6.

1. Introduction

Observations (Feng et al., 2000; Anderson et al., 1996) and model simulations (Schneider and Barnett, 1995; Anderson et al., 1996; Huang and Mehta, 2004, 2005; Huang et al., 2005) suggest that net freshwater input into the oceans may be as important as surface heat flux in contributing to the buoyancy of the upper oceans at seasonal and interannual timescales. There are three types of net freshwater input to the oceans: net atmospheric freshwater (evaporation minus precipitation; EmP), melting sea-ice, and river runoff. Changes in these net freshwater inputs to the oceans can change salinity and, therefore, density of seawater. Changes in density, in turn, can change ocean circulations that can eventually change heat transport and temperature.

Most studies have focused on the role of freshwater in the changes of the Atlantic thermohaline circulation or meridional overturning circulation (MOC; Weaver et al., 1993; Rahmstorf, 1996; Delworth and Greatbatch, 2000; Seidov and Haupt, 2003), although the role of freshwater in the MOC is still under debate (Nilsson et al., 2003; Mohammad and Nilsson, 2004). Sea-ice melting and fresh water export from the Arctic Ocean to the North Atlantic Ocean were recognized to play an important role in the MOC (Weijer et al., 2001; Komuro and Hasumi, 2003; Ottera et al., 2003). Little attention has been paid to the influence of river runoff on currents and temperature. River discharge can induce a return flow that is much larger than the river flow (Huang, 1993), which may subsequently have

*Corresponding author: Boyin HUANG, boyin.huang@noaa.gov

a large influence on ocean currents and temperature changes (Carton, 1991). Recent studies (Huang and Mehta, 2004, 2005; Fedorov et al., 2004; Huang et al., 2005) suggest that thermocline circulations, especially western boundary currents, and temperatures could be significantly affected by changes in EmP at interannual to decadal timescales.

Based on our and other earlier-cited research on the response of ocean circulations and temperature to EmP, we hypothesized that freshwater input to the oceans by rivers can significantly modify the density of seawater near river mouths, which can then modify salt transport and consequently change circulation and heat transport. We tested our hypothesis by conducting several, 500-year long experiments with the global ocean general circulation model (OGCM) developed at the Massachusetts Institute of Technology (MIT). We show that there are significant influences of runoff from major rivers on ocean salinity, circulation, and temperature. We describe the OGCM, river runoff data, and experimental design in section 2. The responses of the oceans to the blocking of the Amazon River are described in section 3. The impacts of blocking runoff from East and South Asian rivers are described in sections 4 and 5, respectively. The results are summarized and discussed in section 6.

2. The MIT OGCM, river runoff data, and experimental design

The MIT OGCM (Marshall et al., 1997; Huang and Mehta, 2004) was used in the present study. The model domain is global from 80°S to 90°N, with realistic topography. The latitudinal resolution is 0.4° near the equator, linearly increasing to a resolution of 2° poleward of 20° in each hemisphere. The longitudinal resolution is 2°. There are 30 levels in the vertical with a resolution of 10 m between the ocean surface and 50-m depth, 25 m between 50- and 200-m depth, 50 m between 200- and 400-m depth, and 50–500 m below 400-m depth. Mesoscale eddies are parameterized by the K-profile parameterization KPP (Large et al., 1994).

Long-term mean monthly runoff from world rivers from Dai and Trenberth (2002) was used in this study. The globally-integrated, annually-averaged freshwater flux from world rivers is approximately 1.25 Sv (1 Sv=10^6 m^3 s^{-1}), with a minimum of 0.95 Sv in December, and a maximum of 1.85 Sv in June (Fig. 1). The runoff from each river in the OGCM is evenly distributed within a box of 50 m in depth and 300 km in the horizontal plane near the river mouth. This is to prevent the model from "crashing" due to dramatic salinity changes in the initial model spinup. The river

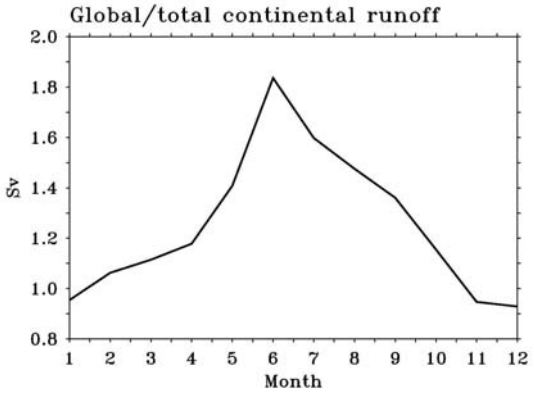

Fig. 1. Globally integrated river runoff. The annually averaged runoff is 1.25, 0.74, 0.31, and 0.14 Sv, respectively, in global, Atlantic, Pacific, and Indian Oceans.

runoff into the ocean is parameterized as a virtual salinity input that acts much like EmP in the model. The heat and momentum associated with runoff are not added to the model oceans.

The OGCM was "spun up" for 400 years from a motionless, initial state of annually-averaged temperature and salinity climatology. During the spinup, the model top-layer salinity was forced by monthly river runoff, precipitation (Huffman et al., 1997), and evaporation (Chou et al., 1997) between 50°S and 60°N. Poleward of 50°S and 60°N, the model top-layer salinity was relaxed to the observed sea surface salinity (SSS) due to a lack of EmP estimates based on observations [see Huang and Mehta (2004) for more details]. The model top-layer temperature was forced by a mixed boundary condition, which consisted of a monthly net heat flux from da Silva et al. (1994) and "relaxation" to monthly, climatological sea surface temperature (SST) with a 10-day relaxation time (50 W m^{-2} K^{-1}). There is no sea-ice in our version of the MIT OGCM, and the minimum ocean temperature was specified at −2°C. Monthly wind stress climatology from Hellerman and Rosenstein (1983) was used, which enabled a more realistic North Equatorial Countercurrent (NECC) simulation. In the spun-up state of the OGCM, the MOC was approximately 22 Sv in the North Atlantic and the Indonesian Throughflow (ITF) was approximately 20 Sv, which are comparable to other OGCM or coupled model simulations cited in section 1.

To test our hypothesis, we first designed a control (CTL) experiment that was conducted with all climatological forcings as used during the spinup. A perturbation experiment (AMZ) was designed by blocking the Amazon River because it has the largest runoff (Table 1) of all rivers. AMZ was conducted with the same forcings as in CTL except that the runoff from

Table 1. Experiments forced by blocking major river runoff. Indonseian Throughflow (ITF) changes in each experiment by year 500 are also listed. Negative ITF anomalies indicate stronger southward ITF.

Exp	Blocked annual discharge (Sv)	Blocked discharge location	Annual ITF anomaly (Sv)
CTL	No blocking	–	–
AMZ	0.28	Amazon region 5°S–5°N	−5.2
CSV	Same as AMZ	Amazon region 5°S–5°N	−3.3
PAC	0.07	East Asia 15°–40°N	0.3
IND	0.09, 0.23 (Aug), 0.02 (Jan)	South Asia 10°–30°N	−0.3

the Amazon River was completely blocked. The complete blocking of river runoff, however, assumes that the blocked freshwater was somehow removed from the Earth-atmosphere system. To evaluate the effect of freshwater conservation while still completely blocking the Amazon River, we designed another experiment (CSV) in which the freshwater due to blocking the Amazon was "precipitated" over the world oceans so that the total freshwater input into the oceans was conserved. The additional precipitation was geographically and seasonally weighted according to the climatological precipitation pattern. To assess the runoff effects of other major rivers on the world oceans, two additional experiments were designed in which the runoff from the East Asian rivers into the western Pacific (PAC), and from the South Asia rivers into the Indian Ocean (IND) was completely blocked. Details of these experiments are listed in Table 1.

After the initial 400 years spinup period, all experiments were run for additional 500 years. Ocean salinity, currents, and temperature were in quasi-equilibrium in the upper oceans at the ends of these experiments. Averaged differences in the last 30 years from year 471 to 500 between the five perturbation experiments and CTL are referred to as anomalies here except where specified otherwise. The last 30 years average was used to remove possible small-amplitude oscillations. The statistical significance of salinity, temperature, and current anomalies was tested using the two-sided student-t method (von Storch and Zwiers,

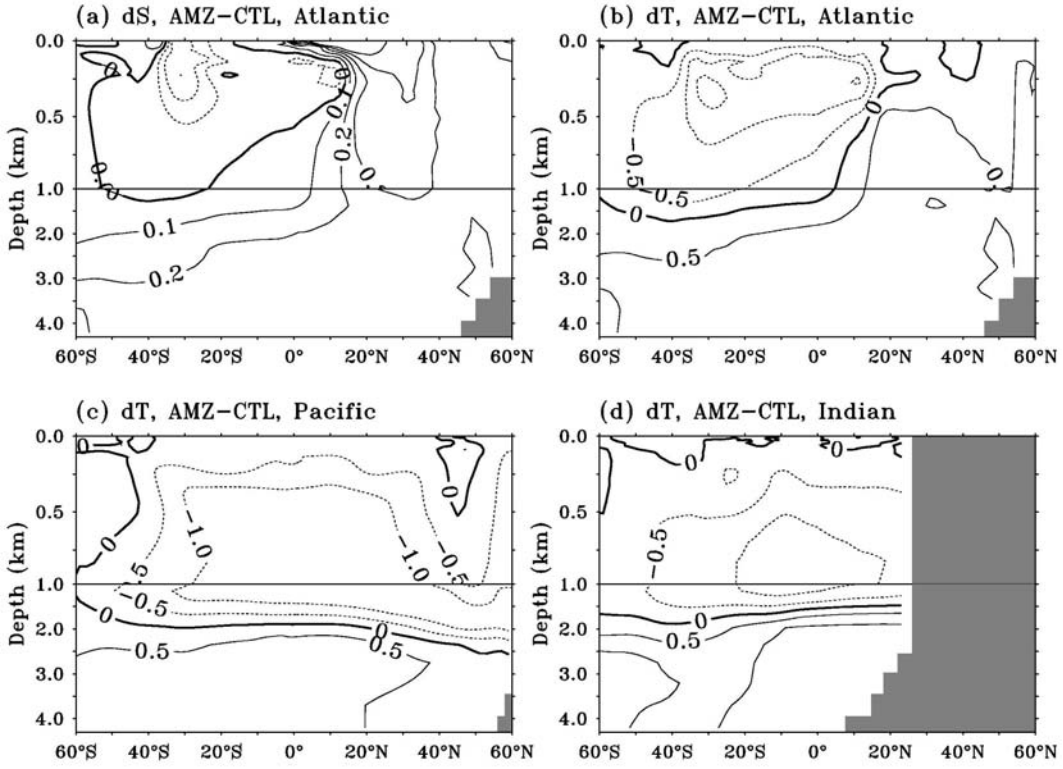

Fig. 2. (a) Zonally-averaged salinity anomaly between AMZ and CTL in the Atlantic. Zonally-averaged temperature anomaly between AMZ and CTL in (b) Atlantic, (c) Pacific, and (d) Indian Oceans. Contour interval is 0.1 psu in (a), and 0.5°C in (b)–(d). Negative values are dashed.

1999). The equivalent number of independent samples was estimated from auto-correlations of anomaly time series at various lags. Only statistically significant results are presented in the following sections.

3. Impacts of the Amazon River runoff

3.1 *Salinity, circulation, and temperature changes in the Atlantic*

In experiment AMZ, the runoff from the Amazon region (0.3 Sv; Table 1) was completely blocked. Because of the blocking, zonally-averaged salinity (Fig. 2a) increased by 0.3–0.5 practical salinity units (psu) in the North Atlantic above 1000 m and 0.1–0.3 psu in the Atlantic below 2000 m. It decreased by 0.1–0.3 psu in the South Atlantic above 500 m. Salinity changes were largely confined near the ocean surface in the western, mainly tropical, North Atlantic (Fig. 3a), where salinity increased by 1.5 psu between the ocean surface and 50 m. The reason for these changes in the North Atlantic was that the saltier water created by blocking the Amazon was transported northward by the Guiana Current and the Gulf Stream. The saltier water was then transported downward by the mean MOC in the extratropical North Atlantic (Fig. 2a).

Zonally-averaged temperature (Fig. 2b) increased by approximately 0.5°C in the North Atlantic below 500 m and in the South Atlantic below 2500 m, and decreased by 0.5°C–1.5°C in the South Atlantic above 1000 m. To understand horizontal structures of temperature and current anomalies, we selected their vertical average between 250 m and 500 m (Figs. 3b and 3c), where zonally-averaged temperature anomalies were large. The structures of these anomalies at other depths (not shown) were similar except for different magnitudes. Temperatures between 250 m and 500 m (Fig. 3b) increased by approximately 0.5°C north of 15°N except near the east coasts of North America and northern South America where temperature decreased by 0.5°C–2°C. Temperature decreased by 1°C–1.5°C in the tropical North Atlantic and South Atlantic between 10°N and 40°S.

It is very interesting to note in Figs. 3b and 3c that temperature changes were clearly associated with changes in ocean currents. The Guiana Current (Fig. 3c) strengthened along the east coasts of Venezuela and northern Brazil. The Gulf Stream strengthened (weakened) off (along) the eastern coast of North America, which is clear in the heat flux anomaly in Fig. 4c. To assess the role of ocean currents in temperature changes, we decomposed total (local) temperature change into longitudinal, latitudinal and vertical advection, and vertical mixing. The temperature change due to horizontal mixing was relatively small and therefore was ignored in our analysis. The various terms in the temperature change equation were averaged from year 1 to year 500 so that anomalous local heat budgets (Fig. 4a) were in a good agreement with temperature anomalies between AMZ and CTL (Fig. 3b).

This diagnostic calculation indicated that the cooling near the east coast of North America (Fig. 4a) was largely associated with anomalous cold advection by eastward anomalous currents (Fig. 4b), and partly associated with anomalous cold advection by southward anomalous currents near the North American coast (Fig. 4c). These anomalous cold advections are consistent with the changes in the Gulf Stream (Fig. 3c). The cooling near the east coast of northern South America was associated with anomalous cold advection by a northward anomalous current (Fig. 4c). The cooling near the east coast of southern South America was associated with anomalous cold advection by both eastward (Fig. 4b) and upward (Fig. 4d) anomalous currents. On the other hand, in the central North Atlantic, anomalous northward currents associated with a stronger Gulf Stream generated anomalous warming (Fig. 4c). In contrast, in the central South Atlantic, anomalous northward currents generated anomalous cooling (Fig. 4c).

Our analyses indicated that anomalous temperature advection resulted from the combination of anomalous currents and climatological temperature gradients. The average temperature between 250 m and 500 m in CTL was shown in Fig. 3c, whose spatial structure was similar to the Levitus et al. (1994) climatology although the average temperature was approximately 1°C–2°C higher than observed climatology (Huang and Mehta, 2005). The zonal gradient of average temperature was positive west of the Gulf Stream axis (Fig. 3c). As the Gulf Stream strengthened, the eastward current strengthened as shown in Fig. 3c. It was the combination of the anomalous eastward current and the positive zonal gradient of average temperature that generated the cooling in the Gulf Stream region. Also, the combination of southward anomalous current and positive meridional gradient of average temperature resulted in the cooling near the coast. In the coastal region of the Guiana Current, the meridional gradient of average temperature was positive (Fig. 3c). As the Guiana Current strengthened, its northward components strengthened. The combination of northward anomalous current and positive meridional gradient of climatological temperature generated the cooling.

These changes in ocean currents, in turn, directly resulted from the changes in salinity and density due to the blocked Amazon River runoff. The strengthen-

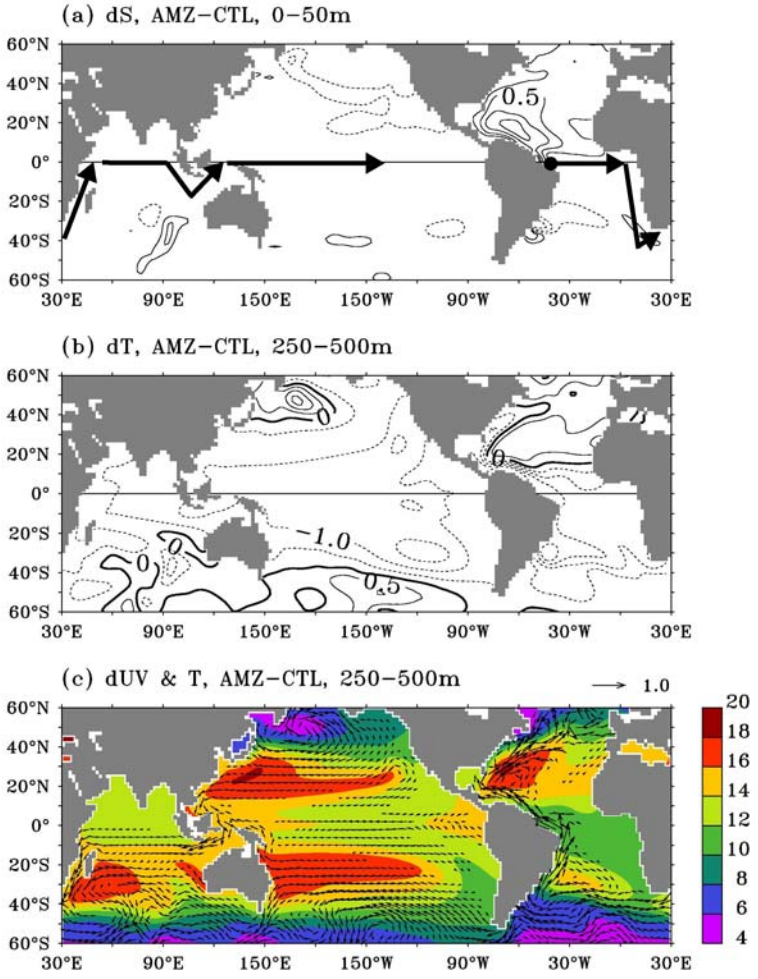

Fig. 3. (a) Salinity anomaly from 0 m to 50 m between AMZ and CTL; contours are ±0.2, ±0.5, ±1, and ±1.5 psu. (b) Temperature anomaly from 250 m to 500 m; contour intervals are 0.5°C. (c) Current anomalies (vectors in 1 cm s^{-1}) and average temperature in CTL (shaded, °C) between 250 m and 500 m. Only vectors larger than 0.05 cm s^{-1} were plotted. Propagations of Kelvin waves are indicated by thick arrows starting from the Amazon region in (a).

ing of the Gulf Stream and the Guiana Current due to the blocked Amazon River runoff were associated with the strengthening of the Atlantic MOC (see Fig. 9) and the global "conveyor-belt" circulation (Broecker, 1991). The current and temperature changes in the Atlantic arising from the blockage of the Amazon River were largely consistent with the results of Ottera et al. (2003) who studied effects of freshwater flux from the Arctic.

3.2 *Circulation and temperature changes in the Indo-Pacific Oceans*

Our results show that the blocking of the Amazon River runoff can cause changes in currents and temperature not only in the Atlantic but also in the Indo-Pacific Oceans due to changes in the Agulhas Current, ITF, South Equatorial Current (SEC), and Equatorial Undercurrent (EUC) (Figs. 3b and 3c). The Agulhas Current strengthened (Fig. 3c), the EUC weakened in the Pacific between 250 m and 500 m (Fig. 3c), and the SEC strengthened in the Indian Ocean (Fig. 3c) and in the Pacific near the surface (not shown). The ITF increased by approximately 5.2 Sv (Table 1) due to blocking the runoff from the Amazon River into the Atlantic Ocean. An anomalous anti-cyclonic gyre was generated in the North Pacific, which might be associated with anomalous upwelling due to stronger conveyor-belt circulation (Broecker, 1991). The subtropical gyre in the South Pacific was also strengthened.

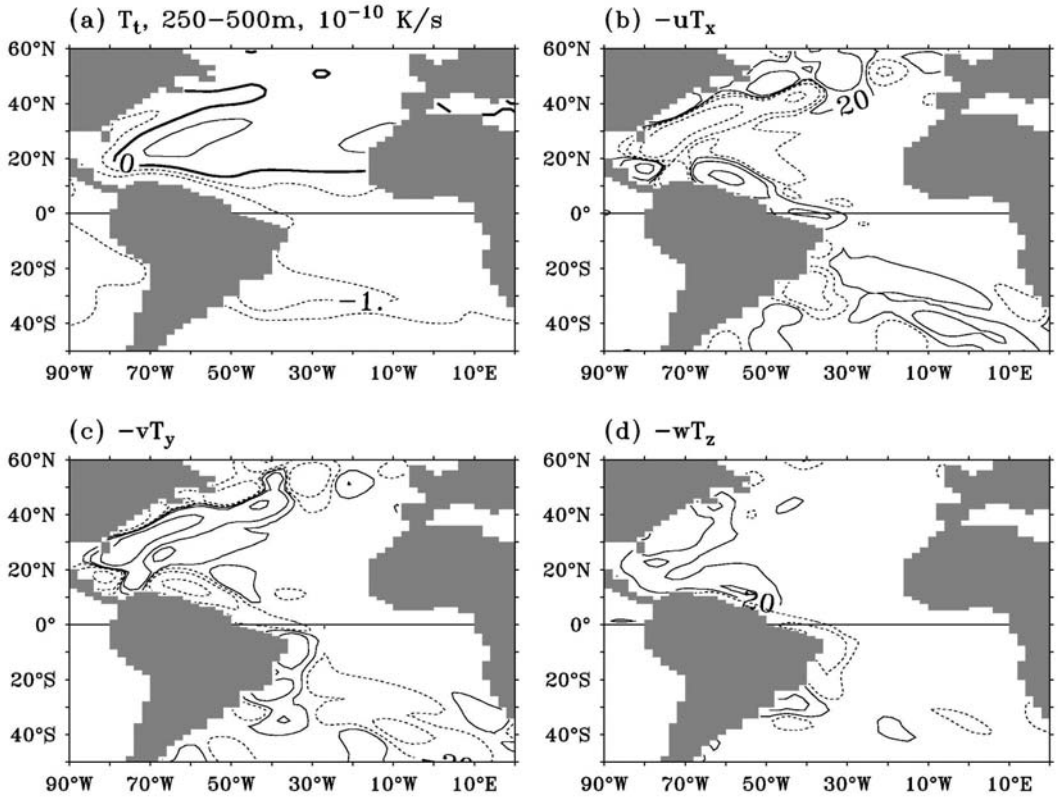

Fig. 4. Average (1–500 year) heat budget anomaly in the Atlantic between AMZ and CTL for (a) local temperature tendency, (b) zonal, (c) meridional, and (d) vertical temperature advection between 250 m and 500 m. Contours are 0, ±0.5, ±1, and ±2 in (a), and ±20, ±100, and ±500 in (b)–(d) (Units: 10^{-10} K s^{-1}). A five-point filter was applied during plotting.

These changes in ocean currents resulted in changes in heat transport and temperature in the Indo-Pacific Oceans. The temperature in the tropical and subtropical Indo-Pacific Oceans (Figs. 2c, 2d, and 3b) decreased by 0.5°C–1°C. The cooling in the subtropical Pacific was associated with enhanced cold advection due to anomalous equatorward currents in the interior subtropical North and South Pacific. The cooling in the tropical Pacific was associated with decreased warm advection due to a weaker EUC and with increased cold advection due to stronger SECs near the ocean surface. In the Indian Ocean, the cooling was largely associated with a stronger ITF and lower temperature in the tropical Pacific (Fig. 3c). Salinity in the upper 50 m of the Indo-Pacific Oceans (Fig. 3a) did not change very much except in the northern North Pacific where anomalous currents were large. The reason is that the anomalous currents did not generate large salt transport due to weaker climatological salinity gradients along the major currents (Huang and Mehta, 2005).

How did anomalous currents and temperature signals propagate from the Atlantic to the Indian and Pacific Oceans? Analyses indicated that transient anomalies of currents and temperature due to blocking the Amazon runoff first propagated eastward along the equator in the Atlantic and then southward along the west coast of southern Africa. After going around the Cape of Good Hope, the anomalies subsequently propagated northward along the east coast of southern Africa and eastward in the Indian Ocean after reaching the equator. These anomalies finally went through the Indonesian passages and propagated eastward in the equatorial Pacific after year 60 of the experiment, which was consistent with the estimate by Cessi et al. (2003). The propagation pathway was clearly indicated by large current anomalies (Fig. 3c) as shown schematically in Fig. 3a.

The eastward propagation pathway from the Indian Ocean to the Pacific Ocean in the AMZ experiment was similar to that due to changes in wind stress according to observations by Clarke and Liu (1993). The propagation direction of temperature and current anomalies was opposite to that of average SECs, the Benguela Current, the Agulhas Current, and the ITF. This indicated that these anomalies did not propagate via mean ocean advection, although the time-mean EUCs in the Atlantic and Pacific may have increased

in eastward propagation speed. The propagation was clearly associated with equatorial and coastal Kelvin waves, as indicated in Cessi et al. (2003) and Huang et al. (2005). The effect of the propagation of these waves was first to change ocean currents and then temperature by anomalous heat advection. Rossby waves are triggered as the equatorial Kelvin waves reached the west coast of Africa, the Indonesian passages and west coast of Australia, and the west coast of South America, as observed by Wijffels and Meyers (2004). Similar interactions between ocean basins via Kelvin waves were also shown by Johnson and Marshall (2004).

3.3 *Redistribution of blocked Amazon River runoff as precipitation*

Experiment AMZ in subsections 3.1 and 3.2 shows that the blocking of the Amazon River lead to changes in circulation and temperature in the Atlantic and Indo-Pacific Oceans. In AMZ, however, the total freshwater input into the oceans was not conserved. To test whether simulated changes of salinity, temperature, and circulation in AMZ were sensitive to the conservation of total freshwater input into the oceans, we designed experiment CSV. In CSV, the freshwater runoff into the Atlantic from the rivers in the Amazon region (0.3 Sv; Table 1) was blocked as in AMZ. The equivalent amount of blocked freshwater was, however, "precipitated" over the world oceans, weighted according to monthly climatological precipitation.

Experiment CSV (not shown) indicated that zonal-average salinity anomalies near the ocean surface in the Atlantic were only slightly weaker than those in AMZ, as shown in Figs. 2a and 3a. The reason is that the freshwater precipitated into the Atlantic was relatively small compared to the reduction of freshwater runoff due to blocking the Amazon River. In the Indo-Pacific Oceans, zonally-averaged salinity decreased due to increased freshwater from additional precipitation. Temperature anomalies in CSV were slightly stronger in the higher latitudes, and slightly weaker in the lower latitudes than those in AMZ, as shown in Figs. 2c, 2d, and 3b. The anomalous anticyclonic flow became slightly stronger in CSV than in AMZ (Figs. 2b and 2c) in the higher latitudes of the North Pacific and South Pacific. These changes were associated with the local input of the excess "precipitation" in the Pacific, according to the Stommel-Goldsbrough circulation hypothesis (Goldsbrough, 1933; Stommel, 1984; Huang, 1993; Huang and Mehta, 2005; Huang et al., 2005). The CSV ex-

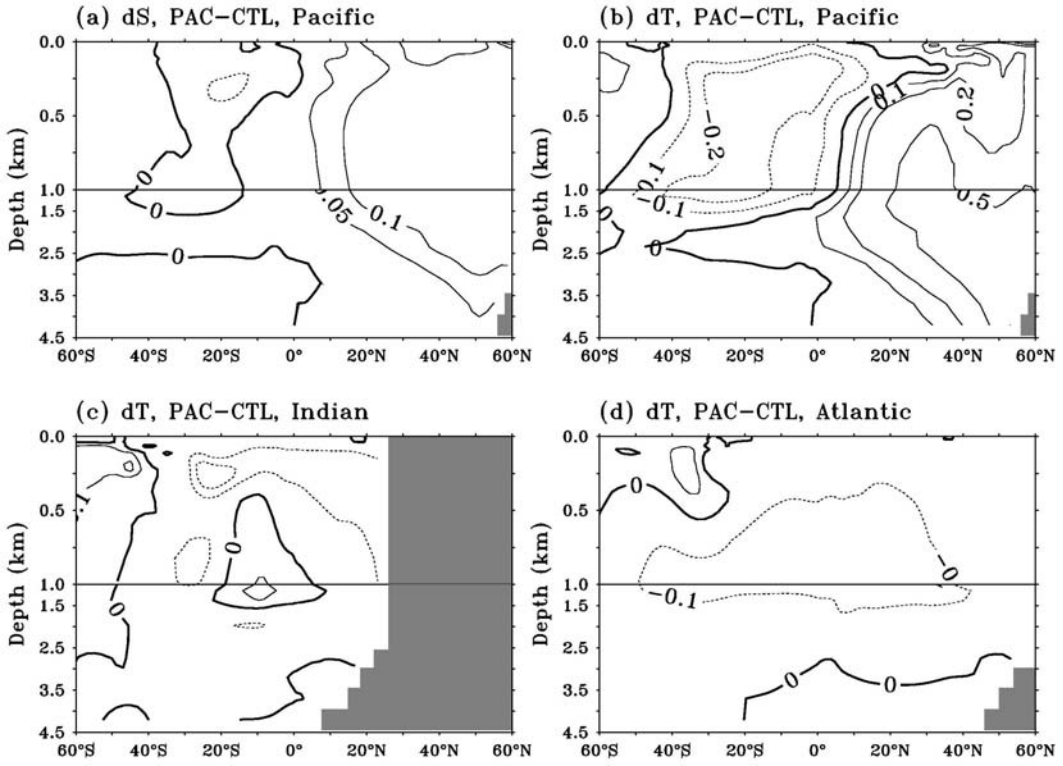

Fig. 5. (a) Zonally-averaged salinity anomaly between PAC and CTL in the Pacific. Zonally-averaged temperature anomaly between PAC and CTL in the (b) Pacific, (c) Indian Ocean, and (d) Atlantic. Contours are 0, ±0.05, ±0.1, and ±0.2 psu in (a), and 0, ±0.1°C, ±0.2°C, and ±0.5°C in (b)–(d).

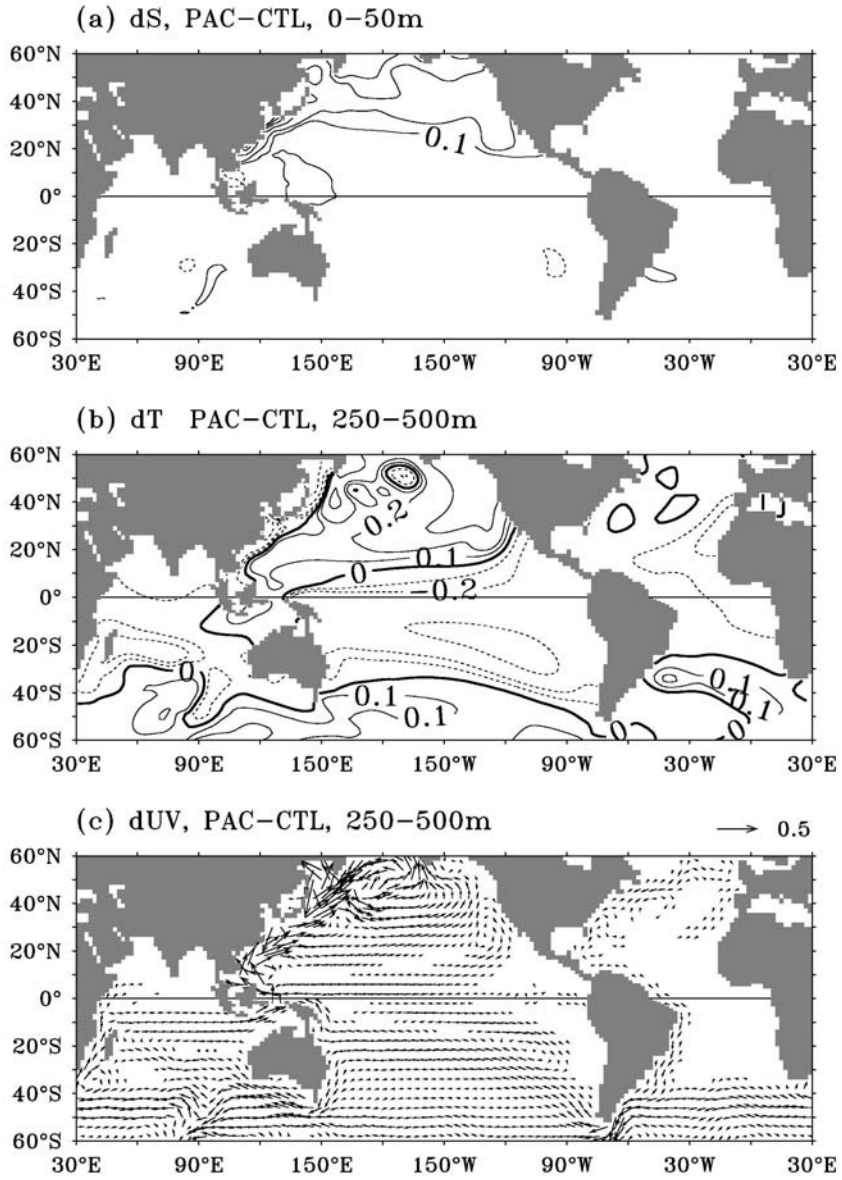

Fig. 6. Same as in Fig. 3 except for anomalies between PAC and CTL. Contours are ±0.1, ±0.2, ±0.5, ±1, and ±1.5 psu in (a), and 0, ±0.1°C, ±0.2°C, and ±0.5°C in (b).

periment showed that the salient features in AMZ were not very sensitive to the conservation of total freshwater input into the oceans. Therefore, to isolate the effect of river runoff, we conducted more experiments to address the impacts of blocked runoff from the East Asian rivers and South Asian rivers without considering total freshwater conservation.

4. Impacts of blocking East Asian rivers

When the freshwater runoff from East Asian rivers (0.07 Sv, largely from the Yangtze River; Table 1) was blocked from the Pacific in experiment PAC, the saltier water was transported to the North Pacific. Zonally-averaged salinity (Fig. 5a) increased by approximately 0.1–0.2 psu in the North Pacific. The salinity increase was largely near the ocean surface and near the east coast of East Asia (Fig. 6a). The saltier water in the North Pacific "spun down" the subtropical gyre, strengthened the SEC, and weakened the EUC, according to the study of Huang and Mehta (2005) and Huang et al. (2005). Due to changes in ocean currents, zonally-averaged temperature (Fig. 5b) increased by 0.2°C –0.5°C north of 10°N, and decreased by 0.1°C–0.2°C between 50°S and 10°N above 1500 m. The temperature between 250 m and 500 m (Fig. 6b) increased

by 0.2°C–0.5°C in the central North Pacific, and decreased by 0.2°C–0.5°C in the tropical and South Pacific between 10°N and 40°S.

Further temperature budget analyses indicated that the warming in the central North Pacific (Fig. 6b) was associated with anomalous warm advection by northeastward anomalous currents (Fig. 6c). The northeastward anomalous currents in the North Pacific were associated with a cyclonic gyre circulation and spin-down of the subtropical gyre according to Huang and Mehta (2005) and Huang et al. (2005). The cooling near the east coast of East Asia resulted from anomalous cold advection. This anomalous cold advection resulted partly from a southward anomalous current (Fig. 6c) east of Japan, and partly from a stronger zonal component of the Kuroshio combined with a positive zonal gradient of average temperature (refer to Fig. 3c). The changes in the western boundary currents and temperature near the east coast of Asia are very similar to those in the Atlantic in experiment AMZ (section 3.1). The cooling in the tropical Pacific resulted from stronger cold advection due to a stronger SEC near the ocean surface, a weaker EUC, and stronger upwelling in the tropical Pacific (not shown). The stronger upwelling in the tropical Pacific was associated with stronger sinking motion in the North Pacific due to higher salinity (and therefore denser) water by blocking East Asian rivers, as proposed by Nof (2001). The cooling in the subtropical South Pacific was clearly associated with anomalous cold advection by northwestward anomalous currents (Fig. 6c). The warming in the Southern Ocean, however, was associated with stronger vertical mixing (not shown).

Our results show that blockage of the eastern Asian rivers into the Pacific can result in changes in temperature and circulation in the Indian and Atlantic Oceans. The tropical Indian Ocean cooled 0.1°C –0.2°C (Figs. 5c and 6b) in PAC compared to CTL. The SEC, the ITF, and the Agulhas Current became weaker (Fig. 6c) due to a weaker density contrast between the Atlantic and Indo-Pacific Oceans. Detailed temperature budget analyses indicated that the cooling in the south Indian Ocean was associated with anomalous cold advection by a weaker Agulhas Current and anomalous northwestward interior flow. The cooling in the Indian Ocean was partly canceled by the warming propagated from the tropical western Pacific by the mean ITF and westward propagating Rossby waves from the Indonesian passages as indicated by Wijffels and Meyers (2004).

Temperature and current anomalies in the Atlantic were weaker (Figs. 5d, 6b, and 6c) due to the smaller freshwater runoff from East Asian rivers in PAC. The temperature between 250 m and 500 m decreased by 0.1°C –0.2°C in the eastern Atlantic between 20°S and 45°N (Figs. 5d and 6b). The weakening of the western boundary currents was barely noticeable.

5. Impacts of blocking South Asian rivers

Experiment IND was designed to study impacts of blocking the runoff from South Asian rivers (0.1 Sv annual average flow; Table 1) into the Arabian Sea

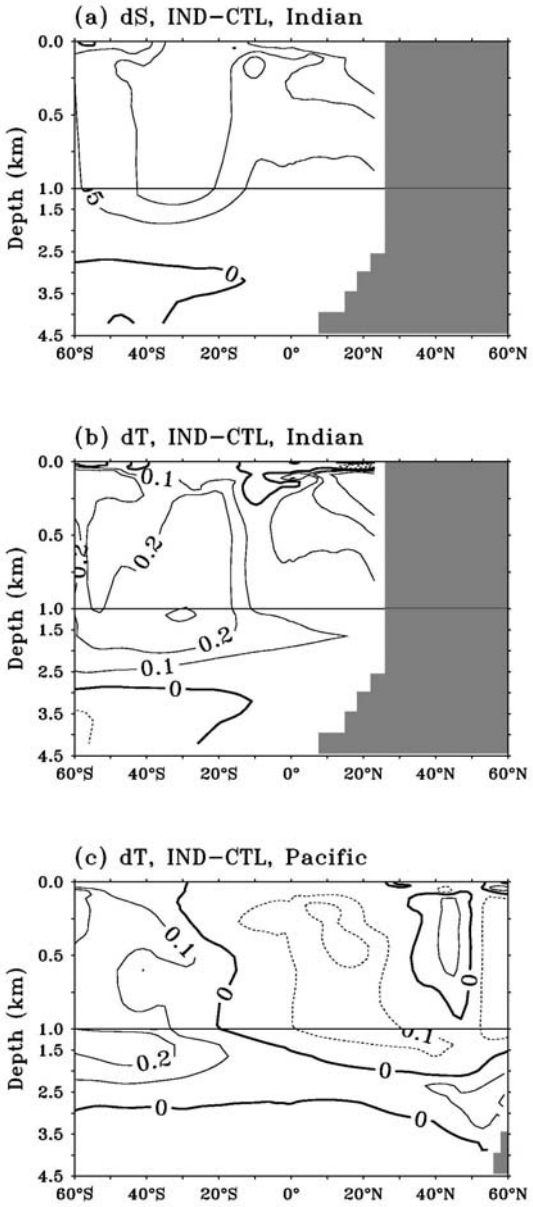

Fig. 7. (a) Zonally-averaged salinity anomaly in the Indian Ocean. Temperature anomalies in (b) Indian Ocean and (c) Pacific Ocean between IND and CTL. Contours are 0, 0.05, 0.1, and 0.2 psu in (a), and 0, ±0.1°C, ±0.2°C, and ±0.5°C in (b) and (c).

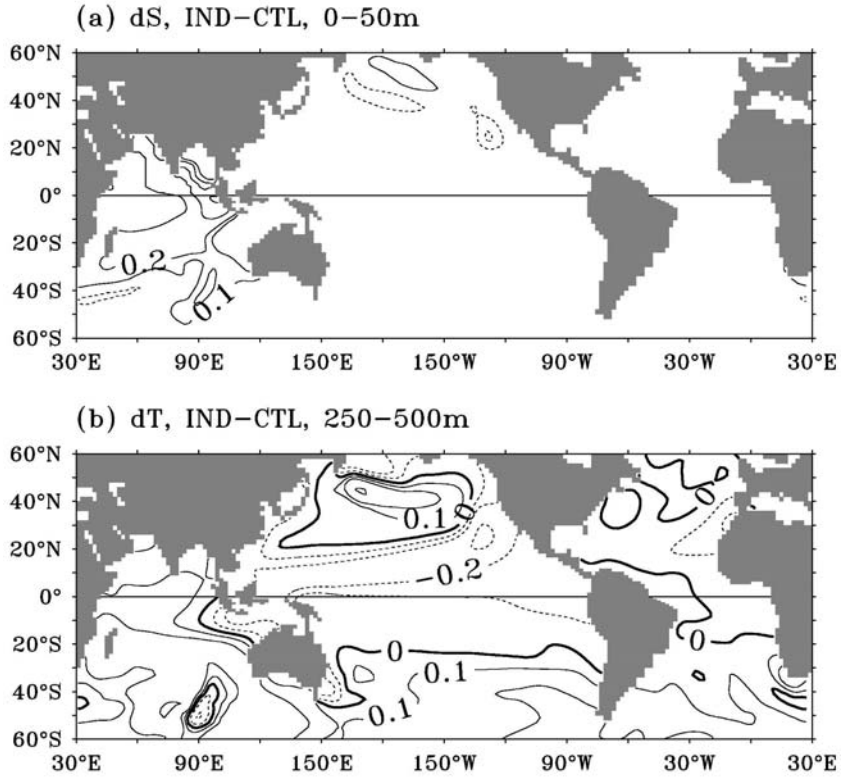

Fig. 8. Same as Fig. 3 except for anomalies between IND and CTL. Contours are ±0.1, ±0.2, ±0.5, ±1, ±1.5, and ±2 psu in (a), and 0, ±0.1°C, ±0.2°C, and ±0.5°C in (b).

and the Bay of Bengal. Due to a strong seasonal variability in river runoff in this region (Table 1), ocean current and temperature anomalies had strong seasonal variability in the north Indian Ocean, but their patterns (not shown) were similar to the annual average. Seasonal variabilities of anomalous currents and temperature due to blocking South Asian rivers were weaker in the Pacific and Atlantic Oceans. Therefore, only anomalies in annual averages were analyzed. IND showed that zonally-averaged salinity (Fig. 7a) increased by 0.1–0.2 psu in the north Indian Ocean above 500 m, and by approximately 0.1 psu between 50°S and 20°S above 1500 m. Salinity anomalies near the surface increased by 0.2–2 psu, but were confined largely within the Bay of Bengal (Fig. 8a). The salinity change in the south Indian Ocean was largely associated with an anomalous salinity "tongue" stretching from the Bay of Bengal and along the SEC.

Zonally-averaged temperature (Fig. 7b) increased by 0.1°C–0.2°C in IND between 200 and 2500 m in the south Indian Ocean and between 100 m and 800 m in the north Indian Ocean. Analysis showed that the warming north of 30°S was associated with anomalous warm advection due to the combined effects of a northward anomalous current (not shown) and the negative meridional gradient of average temperature (Fig. 3c). The warming south of 30°S near 1000 m was largely associated with stronger vertical mixing, which resulted from stronger vertical stratification of temperature due to stronger upwelling to compensate the sinking in the north Indian Ocean.

The warming was relatively deeper and stronger (not shown) in the Arabian Sea than in the Bay of Bengal in IND. Analyses showed that the penetration depth of temperature anomalies might be associated with the direction of average vertical velocity. In the Arabian Sea, average vertical velocity in the MIT OGCM was downward above 500 m because the seawater was saltier from large evaporation; therefore, the warming due to blocking the freshwater runoff into the Arabian Sea was able to penetrate to deeper levels. In contrast, in the Bay of Bengal, the average vertical velocity was upward due to relatively fresher seawater compared to the Arabian Sea, which may have prevented the warming from penetrating to deeper levels.

Our results show that the impacts of blocking freshwater runoff from South Asian rivers can propagate to the Pacific (Fig. 8b), which resulted in a weaker temperature anomaly of 0.1°C–0.2°C in the tropical Pacific between 10°S and 20°N, in the North

Pacific between 30°N and 50°N, and in the Southern Ocean. The temperature changes in the Atlantic were very small.

6. Summary and discussions

Our experiments with the MIT OGCM showed that salinity, currents, and temperature were very sensitive to freshwater runoff from rivers in several regions of the world. Salinity anomalies due to blocking major runoff were as large as 2 psu. The salinity anomalies were largely confined to coastal regions near the ocean surface, but were dispersed by ocean circulations, especially in the Atlantic Ocean. Changes in salinity and therefore density modified the strengths of the Gulf Stream, the Guiana Current, the Kuroshio, the SECs, and the EUCs. The changes in these currents resulted in changes in heat transport and therefore temperature. Temperature anomalies were as large as 1°C – 2°C in the upper oceans, particularly near the east coasts of continents.

The experiments showed that temperature and current anomalies were generated in the Indo-Pacific Oceans by blocking the freshwater runoff from the Amazon River. The propagation of these current and temperature anomalies was caused by coastal and equatorial Kelvin waves. Additional experiments that blocked the Mississippi and Congo Rivers (not shown) generated similar structures but with smaller magnitudes of anomalous temperature and currents in the Atlantic and Indo-Pacific Oceans. This suggests that the oceanic response to the river runoff was not very sensitive to the location of the river as long as it was located within the same ocean basin.

Similarly, withholding freshwater by blocking the river runoff from the Yangtze River into the Pacific could generate temperature and currents anomalies in the Pacific, Indian and Atlantic Oceans, although the anomalies were weaker in the Atlantic. Also, blocking freshwater runoff into the Arabian Sea and the Bay of Bengal could generate anomalous ocean currents and temperature anomalies in the Indian, Pacific, and Atlantic Oceans, although these anomalies were weaker in the Pacific and Atlantic. The results suggest that there can be significant communication among ocean basins via coastal and equatorial Kelvin waves generated due to blocking river runoff.

The basin-scale circulation changes due to blocking freshwater runoff from major rivers were consistent with the hypothetical ocean conveyor-belt circulation (Broecker, 1991), which is believed to be driven largely by density differences between the Atlantic and the Indo-Pacific Oceans. When the density of the upper Atlantic Ocean increased due to blocking river runoff into the Atlantic, both the Atlantic MOC (Fig. 9) and the ITF (Table 1) strengthened. The MOC increased by approximately 8 and 6 Sv, respectively, in the AMZ and CSV experiments. The ITF increased by approximately 5.2, 3.3, and 0.3 Sv in the AMZ, CSV, and IND experiments, respectively. The changes in MOC and ITF indicated the effects of river runoff in global conveyor-belt circulation as proposed by Broecker (1991). In contrast, when the density of the upper Pacific Ocean increased due to blocking the river runoff into the Pacific, both the Atlantic MOC (not shown) and ITF (Table 1) weakened slightly.

In order to study the impacts of blocking runoff from all regions simultaneously, we conducted an additional experiment by blocking all the world's rivers. In this experiment (ALL, not shown), the Atlantic MOC increased by approximately 18 Sv. This is approximately twice the size of the effect from blocking the river runoff of the Amazon region alone (8 Sv, Fig. 9). The effect of blocking all the major rivers on increasing MOC was qualitatively consistent with several previous studies (see for example, Weaver et al., 1993; Rahmstorf, 1996). Another experiment of blocking of all major rivers from Asia into the Pacific Ocean indicated (not shown) that a meridional overturning circulation of larger than 5 Sv could be generated in the Pacific and the temperature can decrease significantly in the upper tropical Pacific Ocean. This suggests the importance of river runoff in correctly simulating the temperature and circulation in the Pacific Ocean.

Since the changes in ocean currents and temperature due to blocking river runoffs involved interactions among the oceans and adjustment of the MOC, the results from 500 years simulation may not fully represent the final changes in ocean equilibrium states, particularly in the deep oceans. We think, however, that changes in the upper 1000 m had already reached quasi-equilibrium states, although the Atlantic MOC

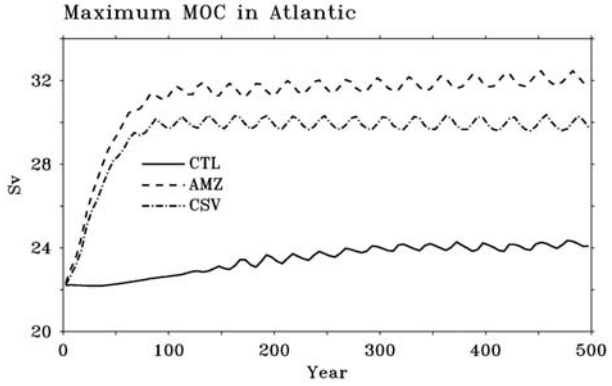

Fig. 9. Maximum MOC (Sv) in the Atlantic in CTL, AMZ, and CSV.

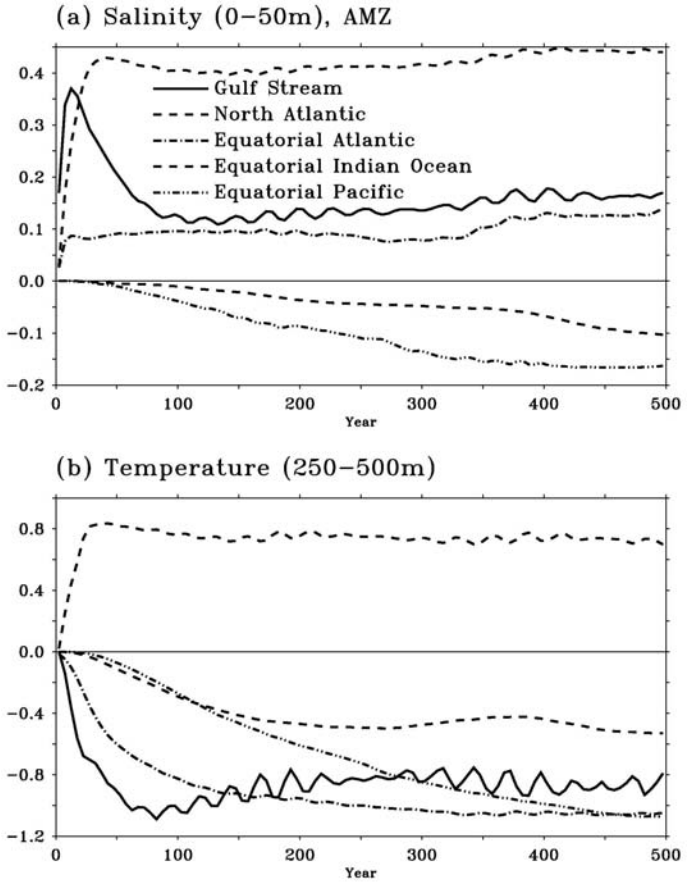

Fig. 10. (a) Salinity anomaly averaged from 0 m to 50 m, and (b) temperature anomaly averaged from 250 m to 500 m between AMZ and CTL. Five regions are located in the Gulf Stream (33°–37°N, 77°–73°W), the North Atlantic (33°–37°N, 43°–37°W), the equatorial Atlantic (4°S–4°N, 23°–17°W), the equatorial Indian Ocean (4°S–4°N, 67°–73°E), and the equatorial Pacific (4°S–4°N, 163°–157°W).

exhibited a weak oscillation at a period of approximately 30 years (Fig. 9). The quasi-equilibrium state can also be seen, for example, in the averaged salinity (0–50 m; Fig. 10a) and temperatures (250–500 m; Fig. 10b) in experiment AMZ in five different regions. The five regions were chosen in the Gulf Stream region (33°–37°N, 77°–73°W), the North Atlantic (33°–37°N, 43°–37°W), the equatorial Atlantic (4°S–4°N, 23°–17°W), the equatorial Indian Ocean (4°S–4°N, 67°–73°E), and the equatorial Pacific (4°S–4°N, 163°–157°W). These regions are located either within the pathways of coastal and equatorial Kelvin waves or in the central Atlantic where the oceans need relatively longer times to reach the equilibrium states. As shown in Fig. 10, salinity and temperature anomalies reached relatively steady states in most regions of the upper oceans by year 500.

It is important to note that model SST in our experiments was forced by combined heat flux and relaxation to observed SST. Therefore, SST anomalies due to blocking major rivers were relatively small in our experiments. Additional experiments showed that the SST anomalies became larger when the SST relaxation coefficient was reduced. Therefore, we speculate that SST anomalies generated by blocking the runoff from major rivers within a fully-coupled ocean-atmosphere system would not be damped strongly as suggested by additional experiments with weaker damping coefficients. We believe that it is reasonable to expect that similar physics may be operating in the actual oceans. But our conclusions need to be confirmed by simulations with coupled ocean-atmosphere models, particularly to assess the magnitudes of changes in salinity, temperature, and Atlantic MOC. An earlier study by Carton (1991) also suggested a strong response in surface salinity and subsurface temperature to changes in

evaporation, precipitation, and river runoff.

Since river runoff can vary at intraseasonal to multidecadal timescales and in response to climate change (see for example, Miller and Russell, 1992), changes in SST due to river runoff may consequently affect regional and/or global climate at various timescales via anomalous air-sea fluxes. Finally, the large temperature changes near the east coasts and the associated anomalous western boundary currents caused by blocking river runoff in our model experiments suggest that a finer model resolution might be helpful to further study the potential influence of river runoff on the coastal salinity, circulation, and temperature changes.

Acknowledgements. This research was supported by NASA grants NAG5-11785 and NAG5-12729. The authors thank A. Dai and K. Trenberth for making the river runoff data available. BH's discussion with P. H. Stone and VM's discussion with T. Delworth are gratefully acknowledged. Comments from two anonymous reviewers helped considerably in improving the description of results of this study.

REFERENCES

Anderson, S. P., R. A. Weller, and R. B. Lukas, 1996: Surface buoyancy forcing and the mixed layer of the western Pacific Warm Pool: Observations and 1D model results. *J. Climate*, **9**, 3056–3085.

Broecker, W. S., 1991: The great ocean conveyor. *Oceanography*, **4**, 79–89.

Carton, J., 1991: Effect of seasonal surface freshwater flux on sea surface temperature in the tropical Atlantic Ocean. *J. Geophys. Res.*, **96**, 12593–12598.

Cessi, P., K. Bryan, and R. Zhang, 2003: Global seiching of thermocline waters between the Atlantic and the Indian-Pacific Ocean basins. *Geophys. Res. Lett.*, **31**, L04302, doi: 10.1029/2003GL019091.

Chou, S.-H., C.-L. Shie, R. M. Atlas, and J. Ardizzone, 1997: Air-sea fluxes retrieved from special sensor microwave imager data. *J. Geophys. Res.*, **102**, 12705–12726.

Clarke, A. J., and X. Liu, 1993: Observations and dynamics of semiannual and annual sea levels near the eastern equatorial Indian Ocean boundary. *J. Phys. Oceanogr.*, **23**, 386–399.

da Silva, A. M., C. C. Young, and S. Levitus, 1994*: Atlas of Surface Marine Data 1994*. NOAA Atlas NESDIS 6-8, U.S. Department of Commerce, NOAA, NESDIS, 83pp.

Dai, A., and K. E. Trenberth, 2002: Estimates of freshwater discharge from continents: Latitudinal and seasonal variations. *Journal of Hydrometeorology*, **3**, 660–687.

Delworth, T. S., and R. J. Greatbatch, 2000: Multidecadal thermohaline circulation variability driven by atmospheric surface flux forcing. *J. Climate*, **13**, 1481–1495.

Fedorov, A. V., R. C. Pacanowski, S. G. Philander, and G. Boccaletti, 2004: The effect of salinity on the wind-driven circulation and the thermal structure of the upper ocean. *J. Phys. Oceanogr.*, **34**, 1949–1966.

Feng, M., R. Lukas, P. Hacker, R. A. Weller, and S. P. Anderson, 2000: Upper-ocean heat and salt balances in the western equatorial Pacific in response to the intraseasonal oscillation during TOGA COARE. *J. Climate*, **13**, 2409–2427.

Goldsbrough, G. R., 1933: Ocean currents produced by evaporation and precipitation. *Proc. Roy. Soc. London*, **A141**, 512–517.

Hellerman, S., and M. Rosenstein, 1983: Normal monthly wind stress over the World Ocean with error estimates. *J. Phys. Oceanogr.,* **13**, 1093–1104.

Huang, B., and V. M. Mehta, 2004: The response of the Indo-Pacific Warm Pool to interannual variations in net atmospheric freshwater. *J. Geophys. Res.*, **109**, C06022, doi: 10.1029/2003JC002114.

Huang, B., and V. M. Mehta, 2005: The response of the Pacific and Atlantic Oceans to interannual variations in net atmospheric freshwater. *J. Geophys. Res.*, **111**, C08008, doi: 10.1029/2004JC002830.

Huang, B., V. M. Mehta, and N. Schneider, 2005: Oceanic response to idealized net atmospheric freshwater in the Pacific at the decadal timescale. *J. Phys. Oceanogr.*, **35**, 2467–2486.

Huang, R. X., 1993: Real freshwater flux as a natural boundary condition for the salinity balance and thermohaline circulation forced by evaporation and precipitation. *J. Phys. Oceanogr.*, **23**, 2428–2446.

Huffman, G. J., and Coauthors, 1997: The Global Precipitation Climatology Project (GPCP) Combined Precipitation Data Set. *Bull. Amer. Meteor. Soc.,* **78**, 5–20.

Johnson, H. L., and D. P. Marshall, 2004: Global teleconnections of meridional overturning circulation anomalies. *J. Phys. Oceanogr.*, **34**, 1702–1722.

Komuro, Y., and H. Hasumi, 2003: Effects of surface freshwater flux induced by sea ice transport on the global thermohaline circulation. *J. Geophys. Res.*, **108** (C2), 3047, doi: 10.1029/2002JC001476.

Large, W.G., J. C. McWilliams, and S. C. Doney, 1994: Oceanic vertical mixing: A review and a model with a nonlocal boundary layer parameterization. *Rev. Geophys.*, **32**, 363–403.

Levitus, S., R. Burgett, and T. Boyer, 1994: *Nutrients.* Volume 3, *World Ocean Atlas 1994*, NOAA Atlas NESDIS 3, U. S. Department of Commerce, Washington, D.C., 99pp.

Marshall, J., A. Adcroft, C. Hill, L. Perelman, and C. Heisey, 1997: A finite volume, incompressible Navier Stokes model for studies of the ocean on parallel computers. *J. Geophys. Res.*, **102**, 5753–5766.

Mohammad, R., and J. Nilsson, 2004: The role of diapycnal mixing for the equilibrium response of thermohaline circulation. *Ocean Dynamics*, **54**, 54–65.

Miller, J. R., and G. L. Russell, 1992: The impact of

global warming on river runoff. *J. Geophys. Res.*, **97**(D3), 2757–2764.

Nilsson, J., G. Brostrom, and G. Walin, 2003: The thermohaline circulation and vertical mixing: Does weaker density stratification give stronger overturning? *J. Phys. Oceanogr.,* **33**, 2781–2795.

Nof, D., 2001: China's development could lead to bottom water formation in the Japan/East Sea. *Bull. Amer. Meteor. Soc.*, **82**, 609–618.

Ottera, O. H., H. Drange, M. Bentsen, N. G. Kvamsto, and D. Jiang, 2003: The sensitivity of present-day Atlantic meridional overturning circulation to freshwater forcing, *Geophys. Res. Lett.*, **30**(17), 1898, doi: 10.1029/2003GL017578.

Rahmstorf, S., 1996: On the freshwater forcing and transport of the Atlantic thermohaline circulation. *Climate Dyn.*, **12**, 799–811.

Schneider, N., and T. Barnett, 1995: The competition of freshwater and radiation in forcing the ocean during El Niño. *J. Climate*, **8**, 980–992.

Seidov, D., and B. Haupt, 2003: Freshwater teleconnections and ocean thermohaline circulation. *Geophys. Res. Lett.*, **30**(6), 1329, doi: 10.1029/2002GL016564.

Stommel, H. M., 1984: The delicate interplay between wind-stress and buoyancy input in ocean circulation: The Goldsbrough variation. *Tellus*, **46A**, 111–119.

von Storch, H., and F. W. Zwiers, 1999: *Statistical Analysis in Climate Research.* Cambridge University Press, 484pp.

Weaver, A., J. Marotzke, P. E. Cummins, and E. S. Sarachik, 1993: Stability and variability of the thermohaline circulation. *J. Phys. Oceanogr.*, **23**, 39–60.

Weijer, W., W. P. E. De Ruijter, and H. A. Dijkstra, 2001: Stability of the Atlantic overturning circulation: Competition between Bering Strait freshwater flux and Agulhas heat and salt sources. *J. Phys. Oceanogr.*, **31**, 2385–2402.

Wijffels, S., and G. Meyers, 2004: An intersection of oceanic waveguides: Variability in the Indonesian Throughflow region. *J. Phys. Oceanogr.*, **34**, 1232–1253.